ELSEVIER

International Journal of Heat and Fluid Flow 22 (2001) 252–258

International Journal of HEAT AND FLUID FLOW

www.elsevier.com/locate/ijhff

Numerical study on turbulent flow and honami in and above flexible plant canopy

Syunsuke Ikeda [a], Tomohiro Yamada [b], Yuji Toda [a,*]

[a] *Department of Civil Engineering, Tokyo Institute of Technology, 2-12-1, O-okayama, Meguro-ku, Tokyo 152-8552, Japan*
[b] *Nippon Steel Co. Ltd., Nishi-Hashimoto, Sagamihara, Kanagawa 229-1131, Japan*

Abstract

The waving of flexible plant termed honami is caused by large-scale vortices which are induced by inflectional instability of flow field. The movement of plant in turn may affect the turbulent flow field via resistance to flow, turbulence production and dissipation. The present study treats the interaction of turbulent flow and honami employing 2D-LES, in which a concept of "plant grid" is used to treat the movement of plant in addition to the ordinary LES grid. The drag due to the plant is formulated in proportion to the square of the relative velocity between flow and motion of plant in momentum equations for turbulent flow field. In transport equation of turbulent energy, the additional terms of turbulent production and dissipation due to motion of plant are included. The computational result indicates that the honami reduces the periodicity of vortex generation, and the velocity fluctuation, therefore, becomes irregular if compared with the case for which the plant is assumed to be rigid. It was also found that the honami repeats generation and disappearance.

Keywords: Honami; Organized vortex; 2D-LES; Flexible vegetation; Interaction

1. Introduction

When wind blows over a flexible plant canopy, a wavy motion of plant termed "honami" is seen to travel downstream. Inoue (1963) first studied such a wavy motion in rice fields and suggested that it is induced by the movement of eddies generated near the top of rice plants.

The recent development of sophisticated devices for measuring turbulence, heat and other substances such as carbon dioxide allows us to observe the large-scale organized vortices in field. For example, Gao et al. (1989) have measured the spatial structure of organized vortices by employing seven triaxial ultrasonic anemometer/thermometers placed vertically in a forest canopy in Canada. They found a 2D coherent structure that consists of a weak ejection from the top of the canopy followed by a strong sweep toward the inside of the canopy. It was also suggested that the wind shear stress near the top of the plant canopy is responsible for the generation of organized vortices. This inference may well be true, because it is known that a shear flow becomes unstable to yield periodic organized vortices if the velocity distribution has an inflectional point (e.g., Tatsumi and Gotoh, 1976; Ikeda and Ohta, 1993). Such a velocity distribution is usually seen near the top of plant canopies.

Shimizu et al. (1992) have used a k–ϵ turbulence model to treat the temporally averaged turbulent flow field in and above a plant canopy. The model has predicted reasonably well the experimentally measured distributions of mean velocity, the turbulence intensity, and the Reynolds stress; it was predicted that the latter two values take the maximum near the canopy top. Kanda and Hino (1994) employed a large-eddy simulation to calculate the growth and the decay of 3D organized vortices generated near the top of the canopy. They predicted that the structure of vortices consists of rollers connected by ribs, as suggested by Hussain (1986). In these numerical computations the plants are assumed to be rigid, and the interaction between the flow and the motion of plant was not treated.

Ikeda and Kanazawa (1996) experimentally studied an open channel flow over a flexible plant canopy, in which the 3D structure of an organized vortex was detected by using particle image velocimetry. They found that the lateral view of the vortex shows an elliptical shape and the vortex is inclined downward towards the front. However, the interaction between the flow and the motion of plant has not been fully understood.

The movement of plant in turn may affect the turbulent flow field via the resistance to flow, the turbulence production and the dissipation. In the present study, a 2D large-eddy simulation including the wavy motion of plant was performed to identify the effect of honami on turbulent flow structure.

* Corresponding author. Tel.: +81-3-5734-2597; fax: +81-3-5734-3577.
E-mail address: ytoda@fluid.cv.titech.ac.jp (Y. Toda).

0142-727X/01/$ - see front matter
PII: S0142-727X(01)00087-X

Notation

A	numerical constant associated with the interaction between flow and motion of plant
b	diameter of plant stalk
C_l	damping coefficient of vibration of a plant stalk
C_D	drag coefficient of a plant stalk
C_M	coefficient of added mass
C_m	drag coefficient of a leaf
C_s, C_e	numerical constants in large-eddy simulation model
d	height of plant
E	Young's modulus of plant
g	gravitational acceleration
I	moment of inertia of plant
k	sub-grid scale kinetic energy
N	number of plants per unit ground area
p	pressure
S	density of leaf area
V_p	volume of plant per unit vertical length
u, w	longitudinal and vertical components of air velocity, respectively
x, z	longitudinal and vertical coordinates, respectively
α	coefficient associated with the velocity distribution in the plant canopy
β	ratio of the transformation of energy loss in a grid scale flow by the drag of plant to the wake production in the sub-grid scale flow
ρ_p	mass density of plant
ρ_f	mass density of air
ν_t	kinematic eddy viscosity
ξ	longitudinal displacement of plant
ζ	longitudinal displacement of the top of plant

2. Governing equations

2.1. Vibration of plants

The movement of plant is assumed to be described by a flexible cantilever. Referring to the coordinate system depicted in Fig. 1, the equation of motion of a flexible plant is written as follows:

$$(\rho_p + C_M\rho_f)V_p\frac{\partial^2\xi}{\partial t^2} + C_l\frac{\partial\xi}{\partial t} + EI\frac{\partial^4\xi}{\partial z^4} = \left(\frac{1}{2}\rho_f C_D b + \rho_f C_m\frac{S}{N}\right)\left(u - \frac{\partial\xi}{\partial t}\right)\left|u - \frac{\partial\xi}{\partial t}\right| + (\rho_p - \rho_f)gV_p\frac{\partial\xi}{\partial z} + \rho_f(1 + C_M)V_p\frac{\partial u}{\partial t} \quad (1)$$

in which ξ is the longitudinal displacement of plant, u the longitudinal component of air velocity, ρ_p the mass density of plant, ρ_f the mass density of air, C_M the coefficient of added mass, V_p the volume of plant per unit vertical length, C_D the drag coefficient of plant stalk, b the diameter of stalk, C_m the drag coefficient of a leaf, S the density of leaf area (total surface area of leaves per unit volume of space), N the number of plants per unit ground area and g is the gravitational acceleration. The first, the second and the third terms in the left-hand side represent inertial term, damping term and bending-stiffness term, respectively. The terms in right-hand side show drag, gravitational force and pressure gradient due to the unsteady motion of fluid, respectively. The drag is formulated in proportion to the square of the relative velocity between the fluid flow and the motion of plant, in which only the longitudinal component of relative velocity is considered, since the vertical component of this is expected to take much smaller value than the longitudinal component.

Since Eq. (1) represents a motion of a plant stalk, the calculation for each plant stalk in the calculation area requires a large computational memory. Therefore, to reduce the computational load, tandem grid systems shown in Fig. 2 were employed. One grid system fixed in space is termed "LES grid" for which the flow velocity, the turbulence energy and the pressure were calculated. Another grid system which moves with the vibration of plants is termed "plant grid", in which the averaged displacement of plants for the grid was calculated. The mass of plants is automatically conserved in the plant grid system.

The longitudinal displacement of plant and the longitudinal component of air velocity in the plant grid are split into

$$\xi = \langle\xi\rangle + \xi^*, \quad (2)$$

$$u = \langle u\rangle + u^* \quad (3)$$

in which $\langle\ \rangle$ denotes the averaged-value for the plant grid, and $*$ indicates the fluctuation from it. Substituting Eqs. (2) and (3) into Eq. (1) and taking average with respect to the plant grid yield

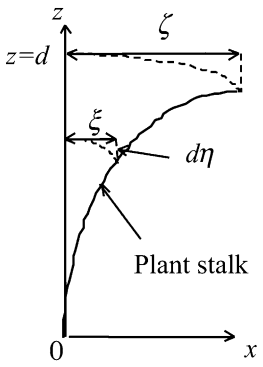

Fig. 1. Coordinate system.

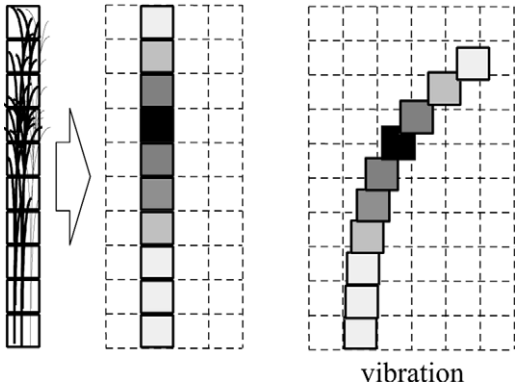

Fig. 2. Tandem grid systems (solid line: plant grid, broken line: LES grid).

$$(\rho_p + C_M\rho_f)V_p\frac{\partial^2\langle\xi\rangle}{\partial t^2} + C_1\frac{\partial\langle\xi\rangle}{\partial t} + EI\frac{\partial^4\langle\xi\rangle}{\partial z^4}$$
$$= \left(\frac{1}{2}\rho_f C_D b + \rho_f C_m\frac{S}{N}\right)\left[\left(\langle u\rangle - \frac{\partial\langle\xi\rangle}{\partial t}\right)\left|\langle u\rangle - \frac{\partial\langle\xi\rangle}{\partial t}\right|\right.$$
$$\left. + \langle u^*u^*\rangle - 2\left\langle u^*\frac{\partial\xi^*}{\partial t}\right\rangle + \left\langle\frac{\partial\xi^*}{\partial t}\frac{\partial\xi^*}{\partial t}\right\rangle\right]$$
$$+ (\rho_p - \rho_f)gV_p\frac{\partial\langle\xi\rangle}{\partial z} + \rho_f(1 + C_M)V_p\frac{\partial\langle u\rangle}{\partial t}. \quad (4)$$

Since Eq. (4) includes the fourth derivative with respect to z in the bending-stiffness term, the numerical calculation for the equation requires very fine resolution in the vertical direction, and therefore the vertical distribution of the displacement of plant is assumed to take a primary mode as derived by the subsequent procedure.

The temporally averaged velocity distribution in the canopy layer is known to take an exponential profile (Inoue, 1963; Ikeda and Kanazawa, 1993). By using this distribution and assuming that the bent of plant is mainly induced by the drag force which is proportional to the square of air velocity, the displacement is described by the following equation:

$$EI\frac{\partial^4\xi}{\partial z^4} = P\exp(2\alpha z) \quad (5)$$

in which P is a proportional coefficient. Integrating Eq. (5) under the boundary conditions for a cantilever, the displacement of primary mode of plant can be obtained. Substituting $z = d$ into the solution, the coefficient P is expressed by

$$P = \frac{48EI\alpha^4}{\exp(2\alpha d)(3 - 6\alpha^2d^2 + 8\alpha^3d^3) - 6\alpha d - 3}\zeta. \quad (6)$$

The displacement of plant, ξ, at height z is expressed by the following equation:

$$\xi(z) = P_s(z)\zeta \quad (7)$$

in which

$$P_s = \frac{3\exp(2\alpha z) - \exp(2\alpha z)(4\alpha^3 - 12\alpha^3z^2d + 6\alpha^2z^2) - 6\alpha z - 3}{\exp(2\alpha d)(3 - 6\alpha^2d^2 + 8\alpha^3d^3) - 6\alpha d - 3}. \quad (8)$$

Integration of Eq. (4) with respect to z from the ground to the top of plant yields

$$(\rho_f + C_M\rho_f)\int_0^d V_pP_s\frac{\partial^2\langle\zeta\rangle}{\partial t^2}\,dz + C_1\int_0^d P_s\frac{\partial\langle\zeta\rangle}{\partial t}\,dz$$
$$+ \int_0^d P\exp(2\alpha z)\,dz = \int_0^d\left(\frac{1}{2}\rho_f C_D b + \rho_f C_m\frac{S}{N}\right)$$
$$\times\left[\left(\langle u\rangle - P_s\frac{\partial\langle\zeta\rangle}{\partial t}\right)\left|\langle u\rangle - P_s\frac{\partial\langle\zeta\rangle}{\partial t}\right| + \langle u^*u^*\rangle\right.$$
$$\left. - 2P_s\left\langle u^*\frac{\partial\zeta^*}{\partial t}\right\rangle + P_s^2\left\langle\frac{\partial\zeta^*}{\partial t}\frac{\partial\zeta^*}{\partial t}\right\rangle\right]dz + (\rho_p - \rho_f)g$$
$$\times\int_0^d V_p\frac{\partial(P_s\langle\zeta\rangle)}{\partial z}\,dz + \rho_f(1 + C_M)\int_0^d V_p\frac{\partial\langle u\rangle}{\partial t}\,dz. \quad (9)$$

The correlation terms in Eq. (9) are estimated by

$$-\langle u^*u^*\rangle = 2\nu_t\frac{\partial\langle u\rangle}{\partial x} - \frac{2}{3}\langle k\rangle, \quad (10)$$

$$-\left\langle u^*\frac{\partial\zeta^*}{\partial t}\right\rangle + P_s\left\langle\frac{\partial\zeta^*}{\partial t}\frac{\partial\zeta^*}{\partial t}\right\rangle = A(-\langle u^*u^*\rangle) \quad (11)$$

in which $\langle k\rangle$ is sub-grid scale (SGS) kinetic energy in the plant grid, ν_t is the eddy viscosity associated with SGS turbulence and A is a numerical constant. Eq. (11) is formulated under a consideration that the displacement of plant is correlated with the fluctuation of air velocity. The value of the numerical constant, A, was determined by a correlation between the rate of displacement of plant and the longitudinal component of velocity fluctuation measured in a reed field (Ikeda et al., 1998).

2.2. Turbulent flow field

The 2D large-eddy simulation is applied to the turbulent flow field. The momentum equations are described by

$$\frac{D\overline{u_i}}{Dt} = -\frac{1}{\rho_f}\frac{\partial\bar{p}}{\partial x_i} + \frac{\partial R_{ij}}{\partial x_j} + \frac{\overline{F_i}}{1 - \bar{c}} \quad (12)$$

in which $\bar{u}_i = (\bar{u}, \bar{w})$ is LES grid-averaged velocity components, $\bar{F}_i = (\bar{F}_x, \bar{F}_z)$ is LES grid-averaged drag force due to plants, R_{ij} is SGS Reynolds stress and $\bar{c}$ is the density of volume of plant. Assuming that the drag force is proportional to the square of relative velocity between air velocity and rate of displacement of plant, the drag force terms, $\bar{F}_i$, are expressed by

$$\overline{F_x} = \left(\frac{1}{2}NC_D b + C_m S\right)$$
$$\times\left[\bar{u}_{rel}\left|\bar{u}_{rel}\right| + \left(\overline{u'u'} - 2P_s\overline{u'\frac{\partial\zeta'}{\partial t}} + P_s^2\overline{\frac{\partial\zeta'}{\partial t}\frac{\partial\zeta'}{\partial t}}\right)\right], \quad (13)$$

$$\overline{F_z} = -\left(\frac{1}{2}NC_D b + C_m S\right)\bar{u}_{rel}^2\frac{\bar{w}}{\left|\bar{u}_{rel}\right|} \quad (14)$$

in which the relative velocity, $\bar{u}_{rel}$, is defined by

$$\bar{u}_{rel} = \bar{u} - P_s\frac{\partial\bar{\zeta}}{\partial t}. \quad (15)$$

The Poisson equation for pressure, $\bar{p}$, is described by

$$\nabla^2\bar{p} = \frac{\partial}{\partial x_j}\left(-\overline{u_i}\frac{\partial\overline{u_i}}{\partial x_j} - \frac{\partial R_{ij}}{\partial x_j} - \frac{\overline{F_i}}{1 - \bar{c}}\right). \quad (16)$$

The transport equation for SGS kinetic energy is written as follows:

$$\frac{Dk}{Dt} = \frac{\partial}{\partial x_j}\left(\nu_t\frac{\partial k}{\partial x_j}\right) + R_{ij}\frac{\partial\overline{u_i}}{\partial x_j} + C_e\frac{k^{3/2}}{\Delta} + P_r - W_T \quad (17)$$

in which C_e is a numerical constant, P_r is SGS energy production rate by the vibration of plant, W_T is the rate of SGS kinetic energy dissipation associated with the drag of plant, and Δ is the grid scale. These variables are described as follows:

$$R_{ij} = -\overline{u_i'u_j'} = \nu_t\left(\frac{\partial\overline{u_i}}{\partial x_j} + \frac{\partial\overline{u_j}}{\partial x_i}\right) - \frac{2}{3}k\delta_{ij}, \quad (18a)$$

$$\nu_t = C_s k^{1/2}\Delta, \quad (18b)$$

$$\Delta = \sqrt{dx\,dz}, \quad (18c)$$

$$P_r = P_{rx} + P_{rz}, \quad (18d)$$

$$W_T = W_{Tx} + W_{Tz}, \quad (18e)$$

$$P_{rx} = \beta\frac{1}{1 - \bar{c}}\left(\frac{1}{2}NC_D b + C_m S\right)\bar{u}$$
$$\times\left(\bar{u}_{rel}\left|\bar{u}_{rel}\right| - P_s\overline{u'\frac{\partial\zeta'}{\partial t}} + P_s^2\overline{\frac{\partial\zeta'}{\partial t}\frac{\partial\zeta'}{\partial t}}\right), \quad (18f)$$

$$P_{\mathrm{tz}} = \beta \frac{1}{1-\bar{c}} \left(\frac{1}{2} N C_{\mathrm{D}} b + C_{\mathrm{m}} S \right) \bar{u}_{\mathrm{rel}}^2 \frac{\bar{w}^2}{\left| \bar{u}_{\mathrm{rel}} \right|}, \tag{18g}$$

$$W_{\mathrm{Tx}} = \frac{1}{1-\bar{c}} \left(\frac{1}{2} N C_{\mathrm{D}} b + C_{\mathrm{m}} S \right) 2k \left| \bar{u}_{\mathrm{rel}} \right|, \tag{18h}$$

$$W_{\mathrm{Tz}} = \frac{1}{1-\bar{c}} \left(\frac{1}{2} N C_{\mathrm{D}} b + C_{\mathrm{m}} S \right) 2k \left| \bar{w} \right| \tag{18i}$$

in which δ_{ij} is Kronecker's delta, C_{s} is a numerical constant, and β is a ratio of the transformation of energy loss in a grid scale flow by the drag of plant to the wake production in the SGS flow. The last two terms in Eq. (18f) are correlated with the velocity fluctuations such that

$$\overline{u' \frac{\partial \zeta'}{\partial t}} + P_{\mathrm{s}} \overline{\frac{\partial \zeta'}{\partial t} \frac{\partial \zeta'}{\partial t}} = A(-\overline{u'u'}), \tag{18j}$$

$$-\overline{u'u'} = 2\nu_{\mathrm{t}} \frac{\partial \bar{u}}{\partial x} - \frac{2}{3} k \tag{18k}$$

in which A is a numerical constant as defined in Eq. (11). For reed field, the thickness of a leaf is about 0.5 mm, the leaf area density is about 7 $\mathrm{m}^2\ \mathrm{m}^{-3}$, and the diameter of a stalk is about 6 mm; thus the volume occupied by plant, $\bar{c}$, is only 0.3%, and therefore it was neglected in the calculation.

2.3. Exchange of properties between LES grid and plant grid

A detail of the grid system is shown in Fig. 3, in which the LES grid is represented by a broken line and the plant grid is expressed by a shaded area. The LES grid and the plant grid are labeled (i, j) and (k, l), respectively. In calculating the flow field, the density of leaf area and the rate of displacement of plant must be distributed from the plant grid to the LES grid. The leaf area density in a LES grid is given by a sum of fractions of the overlapping plant grids on the LES grid, such that

$$S_{i,j} = \sum_{k,l} \gamma_{i,j}^{k,l} S_{k,l} \tag{19}$$

in which $\gamma_{i,j}^{k,l}$ is an overlap ratio between (k, l) grid and (i, j) grid. The rate of displacement of plant in the LES grid is given by

$$\bar{\zeta}_{i,j} = \sum_{k,l} \gamma_{i,j}^{k,l} \frac{S_{k,l}}{S_{i,j}} \langle \zeta_{k,l} \rangle. \tag{20}$$

The flow quantities must be, in turn, fed back from the LES grid to the plant grid in calculating the motion of plant. The grid-averaged flow velocity and the kinetic energy in a plant grid are given by

$$\langle u_{k,l} \rangle = \sum_{i,j}^{i+1,j+1} \gamma_{i,j}^{k,l} \bar{u}_{i,j}, \tag{21}$$

$$\langle k_{k,l} \rangle = \sum_{i,j}^{i+1,j+1} \gamma_{i,j}^{k,l} k_{i,j}. \tag{22}$$

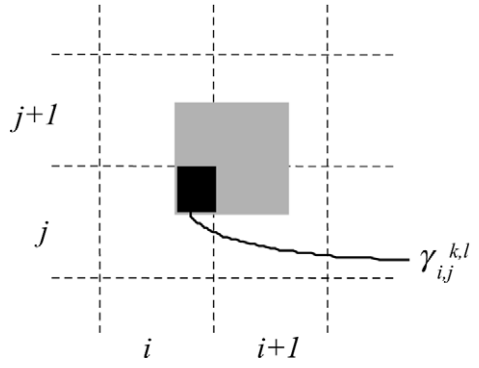

Fig. 3. Enlarged tandem grid systems.

3. Method of computation

The numerical computation was performed for flow observed in a reed field (Ikeda et al., 1998). The area of the calculation was taken to be 50 m in the longitudinal direction and 27.4 m in the vertical direction. The average height of the plant canopy was 2.1 m. The numbers of grid points are 100 in the longitudinal direction and 40 in the vertical direction. The interval of the LES grid is taken to be uniform in the longitudinal direction, and it is not uniform, with finer resolution in the canopy layer, in the vertical direction (Fig. 4). The size of the plant grid is taken to be the same as that of the LES grid in the canopy layer in order to describe correctly the interaction between the flow and the motion of plant. A cyclic boundary condition was used at both the upstream and the downstream ends, and a no-slip condition was employed at the lower boundary. At the upper boundary, a no-slip condition was also used instead of an open boundary condition, since it has not been studied sufficiently for the treatment of turbulence near open boundary. To reduce the effect of the no-slip boundary, the computational domain in the vertical direction is taken to be large enough. Except for the advection terms, which are discretized by the fourth-order upwind difference (e.g.,

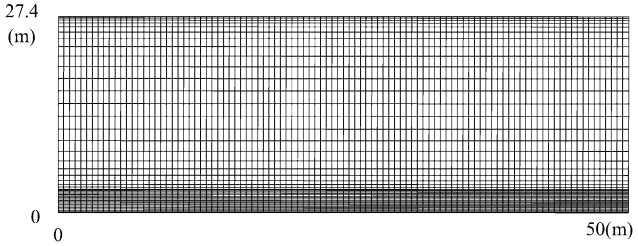

Fig. 4. Computational domain and LES grid system used.

Table 1
Numerical parameters used

	Parameter	Value
Plant	C_{M}	1.0
	EI	1.8 (kg $\mathrm{m}^3/\mathrm{s}^2$)
	C_{l}	1.29 (kg/m s)
	C_{D}	0.1
	C_{m}	0.04
	ρ_{p}	1.6×10^3 (kg/m^3)
	d	2.1 (m)
	b	0.006 (m)
	A	0.01
	N	174 (pieces/m^2)
Fluid	C_{s}	0.05
	C_{e}	1.0
	β	0.1

Kawamura and Kuwahara, 1984), the second-order center difference method was used. The temporal differentiations were approximated by the first-order implicit scheme of the Euler type.

The parameters used in the present calculation are shown in Table 1. The physical properties of plants used are those observed in the reed field (Ikeda et al., 1998). The initial distribution of flow velocity was given by the temporally averaged velocity profile to which a random noise with an amplitude of 1% of the mean velocity was added. The initial distribution of the displacement of plant was assumed to be 0, and the density distribution of leaf area shown in Fig. 5 was given by a polynomial curve obtained by fitting to the observed profile.

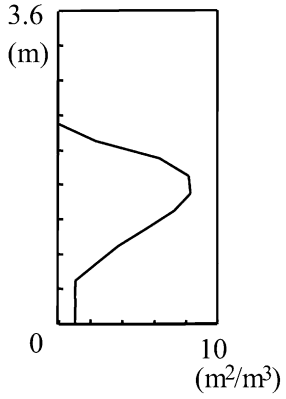

Fig. 5. Initial distribution of density of leaf area.

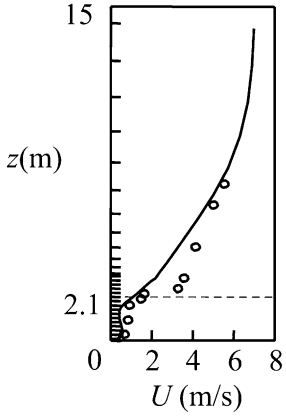

Fig. 6. Temporally averaged velocity field.

4. Results of computation

4.1. Temporally averaged flow field

Fig. 6 shows the vertical distribution of the temporally averaged flow velocity, U, in which the solid line indicates the result of the computation and the open circles represent the values observed in the reed field (Ikeda et al., 1998). The flow velocity is decreased in the canopy layer by the drag due to plants, and the distribution has an inflectional point near the top of the plant canopy. Above the canopy layer, the velocity calculated takes smaller value than the observed values. Though a micro-structure of turbulence in and above the plant canopy is 3D, the major structure of the flow observed by using a thermo-tracer takes 2D profile (Ikeda et al., 1998). Therefore, the present calculation was performed for 2D flow field. The value in the present calculation, $C_s = 0.05$, has been reported to be too large employed in the neighborhood of walls (Horiuti, 1991). This probably yields an over-estimation of eddy viscosity above the canopy layer, which causes a discrepancy between the velocity observed and that of the calculation.

4.2. Temporal fluctuations

Fig. 7(a) shows time series of the displacement of the top of plant canopy, ζ, the temporal fluctuations of longitudinal and vertical velocity components, $\bar{u} - U$ and $\bar{w}$, the SGS Reynolds stress, $-\overline{u'w'}$, and the total Reynolds stress including both the contribution from the grid scale turbulence and the SGS turbulence, $-(\bar{u} - U)\bar{w} - \overline{u'w'}$. The corresponding variables calculated without allowing the vibration of plants are depicted in Fig. 7(b).

At the case without vibration, the temporal fluctuation of flow velocity has a clear periodicity, and the longitudinal and the vertical velocity fluctuations show a negative correlation. A large Reynolds stress is observed during the transition from ejection ($\bar{u} - U < 0$ and $\bar{w} > 0$) to sweep ($\bar{u} - U > 0$ and $\bar{w} < 0$).

On the contrary, the velocity fluctuation computed with allowing the vibration of plants becomes irregular, and the correlation between $\bar{u} - U$ and $\bar{w}$ is not clear. These tendencies are also found in the reed field (Ikeda et al., 1998). The motion of plant, therefore, seems to reduce the periodicity of the organized vortices.

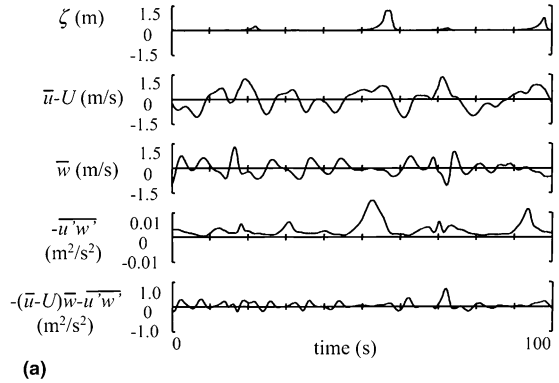

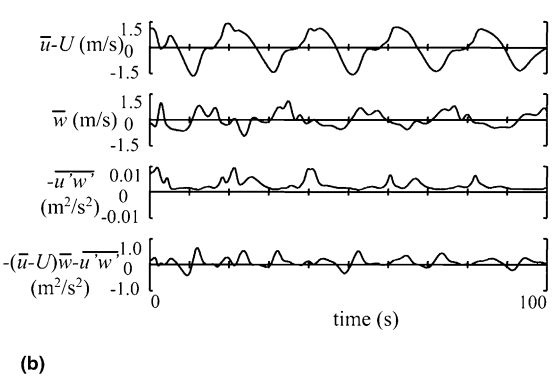

Fig. 7. Time series of various quantities calculated: (a) with allowing the vibration of plants; (b) without allowing the vibration of plants.

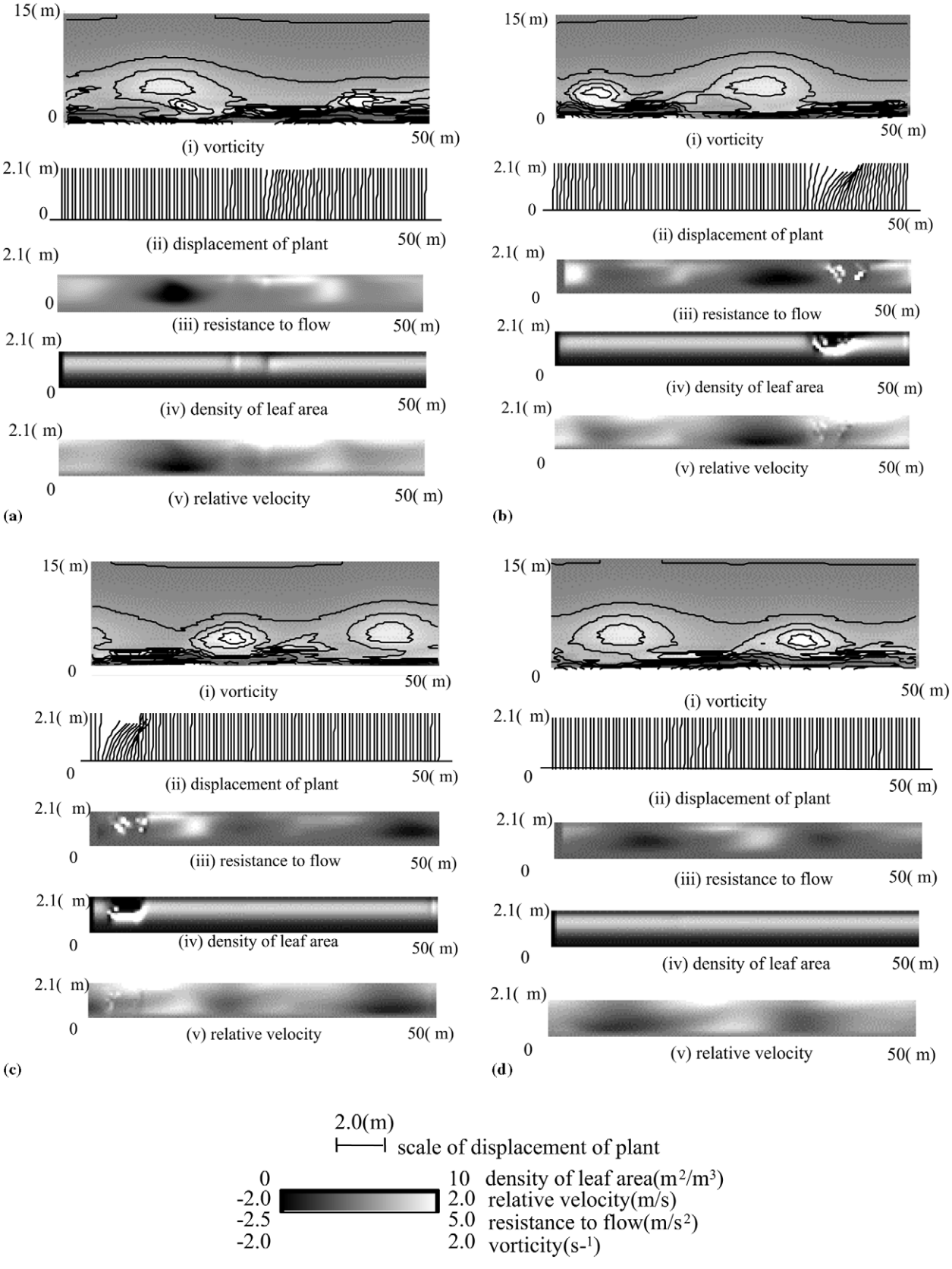

Fig. 8. Instantaneous distributions of various quantities at: (a) $t = 110$ s; (b) $t = 115$ s; (c) $t = 120$ s; (d) $t = 125$ s.

The period of the vortices calculated varies between 10–20 s. The period observed in the reed field was reported to be about 10 s (Ikeda et al., 1998). The reason for the over-estimation of the period may be explained as follows: the longitudinal flow velocity above the plant canopy in the computation takes a smaller value than that in the observation as shown in Fig. 6, and therefore the effect of the vegetation reaches to an area higher than the actual. It suggests that the scale of the vortices computed is larger than that observed in the reed field.

The movement of plant (honami) is found to be induced by stronger vortices. The period of the vibration of plant calculated is about 40 s, and it is about three times of the period of the vortices. In the reed field, the period of honami was observed to be about 30 s, and it is also about three times of the period of the organized vortices (Ikeda et al., 1998). Therefore, the present computation is considered to express the relation between organized vortices and honami reasonably well.

4.3. Interaction between turbulent flow and honami

Fig. 8 shows the instantaneous distributions of vorticity, displacement of plant (honami), resistance to flow, density of leaf area and relative velocity between flow and plant. While vortices are seen in Fig. 8(a), honami does not appear. The reason is explained as follows: the resistance to flow and the relative velocity in front of the large vortex is slightly larger than the ambient area at this moment. Subsequently, a honami is generated at the frontal area of the vortex (Fig. 8(b)). Since the density of leaf area and the relative velocity take large values there, the resistance to flow becomes large. The honami travels downstream with the movement of the vortex (Fig. 8(c)). At the subsequent stage, the relative velocity around the honami is reduced by the increase of resistance to flow, and the honami tends to disappear (Fig. 8(d)). Considering the circumstances mentioned above, the vibration of plant affects the generation of honami via the resistance to flow, which can yield a difference between the period of organized vortices and that of the generation of honami.

5. Conclusions

A numerical study on the interaction between the turbulent flow and the motion of flexible plant was performed, and the results of the calculation have revealed the following:

(1) Honami reduces the periodicity of vortex generation, compared with the case for which the plant is assumed to be rigid.
(2) Honami is intermittent, and it repeats generation and attenuation.
(3) The period of honami is about three times larger than that of the organized vortices.

Acknowledgements

The present study has been conducted under the financial support of Grant-in-Aid for Scientific Research, the Ministry of Education and Culture of Japan (No. 11305035).

References

Gao, W., Shaw, R.H., Pawu, K.T., 1989. Observation of organized structure in turbulent flow within and above a forest canopy. Boundary-Layer Meteorol. 47, 349–377.

Horiuti, K., 1991. On large eddy simulation of turbulent flows, Tenki. Meteorol. Soc. Jpn. 38, 683–697 (in Japanese).

Hussain, A.K.M.F., 1986. Coherent structures and turbulence. J. Fluid Mech. 173, 303–356.

Ikeda, S., Ohta, K., 1993. Instability induced horizontal vortices in shallow open-channel flows. In: Proceedings of the Nineth Symposium on Turbulent Shear Flows, Kyoto, Japan, pp. 14.1.1–14.1.6.

Ikeda, S., Kanazawa, M., 1993. On the velocity distribution in and above flexible plant canopy. In: Proceedings of the 48th Annual Meeting of JSCE, JSCE, No. 2, pp. 718–719 (in Japanese).

Ikeda, S., Kanazawa, M., 1996. Three-dimensional organized vortices above flexible water plants. J. Hydr. Eng., ASCE 122, 634–640.

Ikeda, S., Yamada, T., Sugimoto, T., 1998. An observation on turbulent flow and transports of heat and substances at reed field. J. Hydr., Coastal Environ. Eng., JSCE 593, 79–91 (in Japanese).

Inoue, E., 1963. On the turbulent structure of air flow within crop canopy. J. Meteorol. Soc. Jpn. 1, 317–346.

Kanda, M., Hino, M., 1994. Organized structures in developing turbulent flow within and above a plant canopy, using a large eddy simulation. Boundary-Layer Meteorol. 68, 237–257.

Kawamura, T., Kuwahara, K., 1984. Computation of high Reynolds number flow around a circular cylinder with surface roughness. AIAA paper, 84–340.

Shimizu, Y., Tsujimoto, T., Nakagawa, H., 1992. Numerical study on turbulent flow over rigid vegetation-covered bed in open channels. J. Hydr., Coastal Environ. Eng., JSCE 447, 35–44 (in Japanese).

Tatsumi, T., Gotoh, K., 1976. Stability Theory of Flow. Sangyotosho Publishing Company, Chiyoda, Tokyo (in Japanese).